A Compact Implantable Antenna for Bio-Telemetry

Sumyea Sabrin, Karu P. Esselle, and Khaled Mahbub Morshed
Department of Engineering, Macquarie University, Sydney, NSW 2109, Australia
Email: Sumyea.Sabrin@mq.edu.au, Karu.Esselle@mq.edu.au, Khaled.M.Morshed@ieee.org

***Abstract*—A compact implantable planar inverted-F antenna with the full ground plane is presented for bio-telemetry applications in the medical device radiocommunications service (MedRadio) band (401 - 406 MHz). A basic three layer phantom model of skin, fat and muscle is initially considered and the antenna is placed in the muscle layer. Later, Gustav voxel model is used to verify the design. The overall size of the antenna is 11.635 × 11.635 × 1.975 mm^3, equivalent to 0.0156λ_o × 0.0156λ_o × 0.00266λ_o (here, λ_o is the free space wavelength at 403.5 MHz). The antenna has an impedance bandwidth of 2.73% (397.4 - 408.4 MHz) with a voltage standing wave ratio of 2:1 and peak realized gain of -29.6 dBi at 403 MHz. The estimated maximum SAR value of this antenna satisfies the IEEE and FCC standard safety guidelines for 1-g and 10-g average SAR at 403 MHz, allowing 3.37 mW and 27.05 mW maximum input power, respectively.**

Keywords*—Implantable antenna, MedRadio band, implantable medical devices (IMDs), specific absorption rate (SAR).

I. Introduction

Implantable medical devices (IMDs) have recently attracted significant scientific interest for many diagnostic and therapeutic applications because of the growing concerns of human health, aging populations and the convenience of medical care [1]–[4]. In a typical bio-telemetric system, bio-signals are wirelessly transmitted from inside the human body to an external receiver over a distance of a few meters [5], [6]. To make this wireless communication with the external pieces of equipment, an implantable antenna is necessary. The operating frequencies of the implantable medical devices (IMDs) are usually in the MedRadio band (401-406 MHz) with a 1.24% bandwidth. The challenge is that the loss and asymmetric features of the human body degrade antenna radiation efficiency and pattern. On the other hand, implantable antennas have to be compact in size and resonate at a relatively low frequency band [5], [7], [8]. So, size reduction is the most important challenge for an implantable antenna in view of minimizing the discomfort caused by IMDs [9].

Many implantable antennas have been designed with different strategies and types. A conformal spiral type Implantable antenna at Medical Implanted Communication Service (MICS) band has been designed with applying the recently proposed mideld wireless power transfer (WPT) technique at 1.5 GHz to avoid the telemetry problem and bulky energy storage component [10]. An implantable Hilbert curve fractal antenna is designed by employing differentially fed and fractal technologies to suit the differential circuitries of radio frequency integrated circuits (RFICs) and to minimize the size of the antenna, respectively [11]. A radiation pattern reconfigurable antenna for medical implants is designed where Two artificial switches have been employed to perform a radiation pattern reconfigurable property and miniaturization is achieved by spiraling a monopole antenna [12]. Employing active radio-frequency identification (RFID) technology, existing ultra-high frequency (UHF) telemetry system operating in free space, has been converted into an implantable telemetry system and the antenna size is reduced by using two placements options: on the ground-plane side and on the component-side of the tag so that it suits the space available in the active RFID tag [3].

Some of the relevant miniaturization techniques are the use of high permittivity substrate, patch meandering, as well as shorting pin loading [13]. With the use of meandering and shorting strategy, the whole dimension (including the superstrate) of the proposed antenna has been signicantly reduced [9]. Employing high permittivity substrates and adopting a slow wave structure such as adding shorting pins in close proximity to the feeding probe, and loading parasitic elements size reduction has been realized [2]. The compactness of the antenna is achieved effectively by optimally canceling its inherent high capacitance through L-shaped reactive loading sections within the antenna structure [14]. Effective size reduction at a fixed frequency operation can be obtained by embedding three arc-shaped slots in a semicircular patch [1]. A modified planar Inverted-F Antenna with stacked structure (three layers with a ground, lower patch, and upper patch) is designed that extends the current path effectively, miniaturizing the antenna dimensions [15].

In this paper, we focus on the compactness of the antenna for implantable bio-telemetry application at MedRadio band. We consider single layer substrate with the full ground plane and meandering line with a shorting to achieve the compact size. After geometrical dimension optimization using CST microwave studio, the proposed antenna occupies a compact size of 11.635 × 11.635 × 1.975 mm^3 and a bandwidth of 2.73%. The manuscript is organized as follows: Section II presents the configuration of the proposed antenna together with three layers phantom model consideration. Section III presents the predicted results using three layer phantom model and using Gustav voxel model [16], followed by the conclusion in Section IV.

II. Antenna Configuration

Our aim to design an implantable antenna with compact size, having acceptable gain and radiation. We choose a planar inverted-F antenna because of its simple structure and small size. The antenna is designed and simulated using CST microwave studio. In our design, we have considered full ground plane and a high dielectric substrate. The top view, side view, and bottom view of the proposed implantable compact antenna are shown in Fig. 1. To design implantable antenna Rogers TMM 10i (ϵ_r = 9.8, and $tan\delta$ = 0.002) is considered as substrate with a dimension of 11 × 11 mm^2. Teflon box,

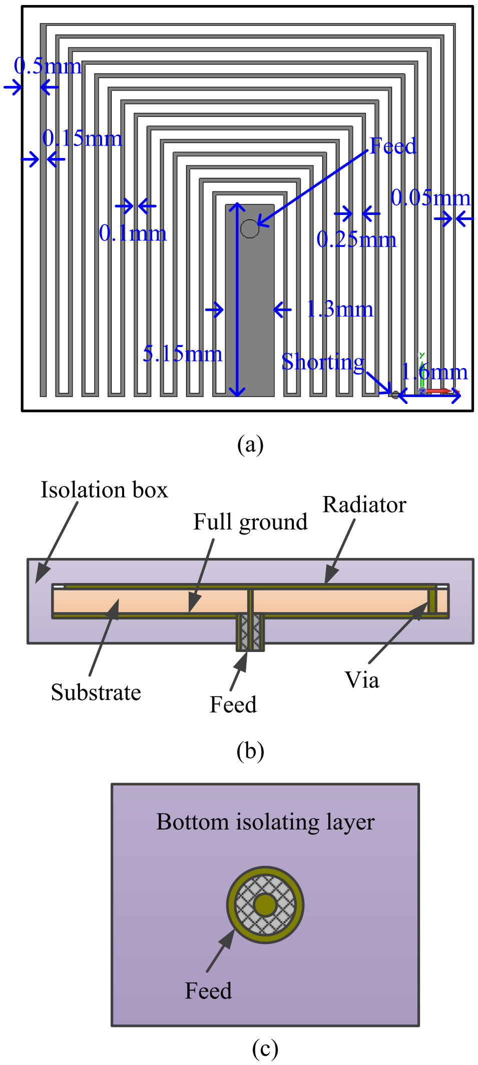

Fig. 1: Proposed implantable antenna structure: (a) top view, (b) side view, and (c) bottom view.

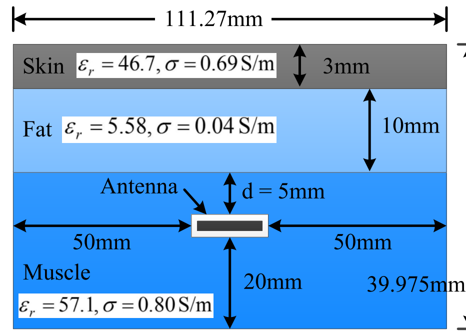

Fig. 2: Three layer phantom model used in CST microwave studio and the antenna placement.

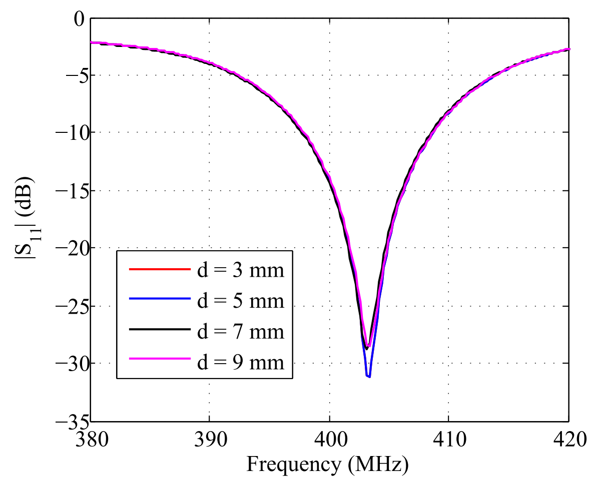

Fig. 3: Reflection coefficient frequency response of the antenna. Here, d is the distance between the antenna and the bottom layer of fat.

a thickness of 0.635 mm, is used to isolate the surrounding tissues from the metal radiator. The dimension of the ground plane is 11 $\times$ 11 mm^2. The main structure of the antenna is square shaped meandered radiating element and feeding is provided at the center of the structure. The thickness of the meandered line/radiator is 0.1 mm and gap between two radiating lines is 0.25 mm. However, a different thickness is considered at the edge side of the antenna for tuning the resonance of the antenna and the thickness are 0.05 mm and 0.15 mm, shown in Fig. 1. A shorting pin is used for further compactness and as well as to tune the antenna resonance. The radius of the shorting pin is 0.1 mm. Location of the shorting pin are depicted in Fig. 1. The antenna is feed with a coaxial probe from the bottom side as depicted in Fig. 1(c).

A three-layer cubic phantom model containing skin, fat, and muscle has been considered in this design. The antenna is placed in the muscle layer of the phantom model and the placement of the antenna with respect to three layer phantom model is shown in Fig. 2. The antenna is placed 5 mm away from the fat layer and the whole size of the phantom model is 111.27 $\times$ 111.27 $\times$ 39.975 mm^3. The impact of the different distance placement of the antenna from the fat layer are presented in Section III. The thickness and dielectric properties of different tissues at 403 MHz are collected from [17]. After that, Gustav voxel model [16] has been considered to verify the design. For practical engineering, the antenna is placed in the muscle layer covered by a bio-compatible material layer and re-tuning may require when this layer is consider for simulation. In our design, we only focus on antenna design that will be placed into the muscle layer. To reduce the effect of muscle we encapsulate the antenna by low dielectric constant material.

III. Results and Discussion

Simulation of the proposed antenna has been carried out using the optimized geometry of the antenna (shown in Fig 1) and the three layer phantom model (shown in Fig. 2). The antenna is placed on the muscle layer and placed at 5 mm away from the bottom layer of the fat. The antenna resonated at 403.4 MHz, and the antenna has the return loss bandwidth of 11 MHz (397 - 408 MHz) covering the MICS/MedRadio band, shown in Fig. 3. The antenna reflection coefficient frequency response for different distant placement e.g. d = 3 mm, d

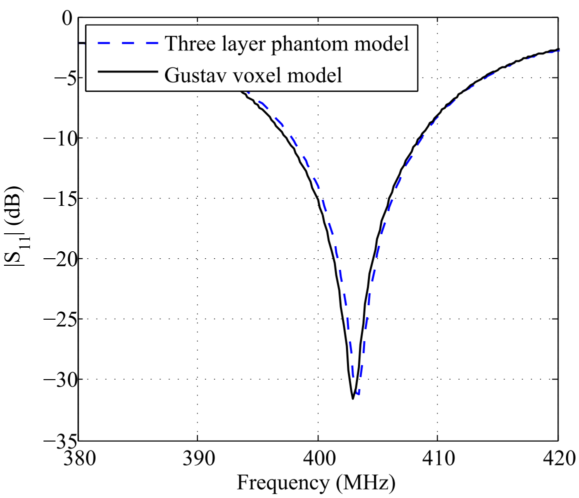

Fig. 4: Reflection coefficient frequency response of the antenna calculated in the three layer phantom model and the Gustav voxel model.

TABLE I: Maximum SAR value calculated, with 1 W input power, in Gustav voxel model and Maximum allowable input power at 403 MHz.

Standard	Max SAR (W/Kg)	Max input power (mW)
C95.1-1999 (1-g avg)	475.068	3.37
C95.1-2005 (10-g avg)	73.933	27.05

= 5 mm, d = 7 mm, and d = 9 mm are shown in Fig. 3. The proposed antenna exhibits relatively stable impedance behavior for different positioning as shown in Fig. 3. As the antenna surrounded by a low dielectric constant substrate, change in installation depth has negligible effect on the antenna reflection coefficient behaviour. Now we verify the design by placing the antenna in Gustav voxel model. The antenna is implanted into the chest of Gustav voxel model and the return loss is shown in Fig. 4. Slight de-tuning is observed and the resonance of the antenna is shifted to 403 MHz. The impedance bandwidth is 11 MHz (397.4 - 408.4 MHz) that is still covering the MedRadio band. Possible reasons for the slight de-tuning are the skin surface in three layer phantom model is homogeneous but in case of Gustav voxel model, the skin surface is nonhomogeneous. As the antenna is covered with 0.635 mm thin Teflon box, significant de-tuning has not been observed. In further analysis or result calculation, we consider Gustav voxel model.

Considering 1 W input power simulated maximum 1-g and 10-g SAR values are 475.068 W/Kg and 73.933 W/kg at 403 MHz, respectively. According to FCC and IEEE, the expected/allowed SAR values for wearable or implantable medical devices, to protect the patients from the damage of electromagnetic radiation, are 1-g average SAR is less than 1.6 W/kg and 10-g average SAR is less than 2 W/kg [18]–[20]. Therefore, the maximum allowable input power of the antenna is limited by the standard and are presented in Table I.

The proposed antenna has the directivity of 2.62 dBi and the maximum realized gain is -29.6 dBi at 403 MHz. The

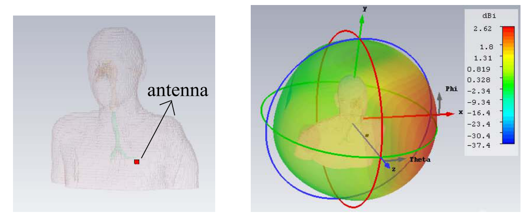

(a) (b)

Fig. 5: Implantable antenna in the Gustav voxel model (a) Implanted site, and (b) 3-D directivity radiation pattern at 403 MHz in the Gustav voxel model.

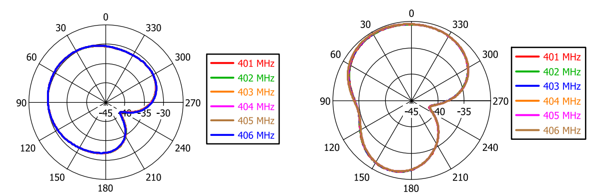

(a) (b)

Fig. 6: Antenna radiation pattern in (a) xz plane, and (b) yz plane.

antenna implantation site and 3-D directional radiation pattern at 403 MHz has been presented in Fig. 5. Because of being the long current path, the realized gain of the proposed antenna is higher. The radiation pattern of the antenna in xz and yz plane with the variation of operating frequency in a step of 1 MHz are shown in Fig. 6. The radiation pattern is in broadside over the whole MedRadio band. Here we see that the radiation pattern is stable with the change of the operating frequency. Finally, in Table II we have compared the gain of the proposed antenna to other implantable antenna, with the full ground plane for bio-telemetry applications found in recent literature. From the comparison, we see that the gain of our proposed implantable antenna is higher and acceptable.

IV. Conclusion

In this paper, a compact PIFA antenna is presented for implantable medical devices. The antenna impedance bandwidth covers 403 MHz MICS/MedRadio band. Detailed design considerations for the antenna are described. The antenna has a single layer substrate backed by full ground plane. The

TABLE II: Gain comparison of MedRadio band implantable antennas with full ground planes.

Reference	Antenna	Max gain (dBi)
[1]	PIFA	-33.2
[9]	PIFA	-32.49
[14]	Planar Dipole	-29.4
[15]	PIFA	-36.48
Proposed	PIFA	-29.6

single layer structure is easier to fabricate, robust to package environment and inexpensive. For isolating the radiator and ground plane from the biological tissues, the antenna is covered with a 0.635 mm thick Teflon box. The antenna designed using a simplified three layer phantom model was verified using Gustav voxel model. The radiation pattern of the antenna was stable over the MICS/MedRadio band and direction of radiation is in broadside. The maximum SAR value satisfies IEEE and FCC standard safety guidelines.

ACKNOWLEDGMENT

The authors would like to thank, *Foundation for Research on Information Technologies in Society*, Zeuhausstrasse 43, 8004 Zurich, Switzerland for their model and voxel files, and the virtual family tool software.

REFERENCES

[1] S. Q. Xiao and R. Q. Li, "Antennas design for implantable medical devices," in *IEEE International Conference on Computational Electromagnetics (ICCEM)*, Feb. 2015, pp. 61–63.

[2] L.-J. Xu, Y.-X. Guo, and W. Wu, "Miniaturized circularly polarized loop antenna for biomedical applications," *IEEE Trans. Antennas Propag.*, vol. 63, no. 3, pp. 922–930, Mar. 2015.

[3] M. S. Islam, K. P. Esselle, D. Bull, and P. M. Pilowsky, "Antenna design and placement options for an implantable wireless medical telemetry system," in *IEEE Antennas and Propagation Society International Symposium (APSURSI)*, Jul. 2014, pp. 512–513.

[4] ——, "Implantable compact antennas for wireless bio-telemetry: A comparative study," in *International Workshop on Antenna Technology: "Small Antennas, Novel EM Structures and Materials, and Applications" (iWAT)*, Mar. 2014, pp. 167–170.

[5] R. S. Alrawashdeh, Y. Huang, M. Kod, and A. A. B. Sajak, "A broadband flexible implantable loop antenna with complementary split ring resonators," *IEEE Antennas Wireless Propag. Lett.*, vol. 14, pp. 1322–1325, 2015.

[6] M. S. Islam, K. P. Esselle, D. Bull, and P. M. Pilowsky, "A miniaturized implantable pifa antenna for indoor wireless telemetry," in *IEEE International Conference onElectromagnetics in Advanced Applications (ICEAA)*, Sep. 2012, pp. 526–530.

[7] M. S. Islam, K. P. Esselle, L. Matekovits, D. Bull, and P. M. Pilowsky, "An implantable pifa antenna with a j-shaped proximity feed for rfid telemetry," in *IEEE International Conference on Applied Electromagnetics and Communications (ICECom)*, Oct. 2013, pp. 1–4.

[8] ——, "An implantable hilbert pifa antenna for rfid based telemetry," in *IEEE International Conference on Electromagnetics in Advanced Applications (ICEAA)*, Sep. 2013, pp. 790–793.

[9] H. Li, Y. X. Guo, C. Liu, S. Xiao, and L. Li, "A miniature-implantable antenna for medradio-band biomedical telemetry," *IEEE Antennas Wireless Propag. Lett.*, vol. 14, pp. 1176–1179, 2015.

[10] R. Das and H. Yoo, "Biotelemetry and wireless powering for leadless pacemaker systems," *IEEE Microw. Wireless Compon. Lett.*, vol. 25, no. 4, pp. 262–264, Apr. 2015.

[11] H. Liu and X.-Y. Liu, "A miniaturized differentially fed implantable hilbert curve fractal antenna at mics band," in *IEEE International Conference on Computational Electromagnetics (ICCEM)*, Feb. 2015, pp. 275–277.

[12] V. T. Nguyen and C. W. Jung, "Radiation-pattern reconfigurable antenna for medical implants in medradio band," *IEEE Antennas Wireless Propag. Lett.*, vol. PP, no. 99, pp. 1–1, 2015.

[13] A. Kiourti and K. Nikita, "A review of implantable patch antennas for biomedical telemetry: Challenges and solutions [wireless corner]," *IEEE Antennas Propag. Magn.*, vol. 54, no. 3, pp. 210–228, Jun. 2012.

[14] S. Bakogianni and S. Koulouridis, "An implantable planar dipole antenna for wireless medradio-band biotelemetry devices," *IEEE Antennas Wireless Propag. Lett.*, vol. PP, no. 99, pp. 1–1, 2015.

[15] Z. Wu, X. Liu, and Y. Di, "A novel stacked inverted-f antenna for implanted bio-devices in the mics band," in *IEEE International Conference on Computational Electromagnetics (ICCEM)*, Feb. 2015, pp. 355–357.

[16] A. Christ, W. Kainz, E. G. Hahn, K. Honegger, M. Zefferer, E. Neufeld, W. Rascher, R. Janka, W. Bautz, J. Chen, B.Kiefer, P. Schmitt, H. P. Hollenbach, J. Shen, M. Oberle, D. Szczerba, A. Kam, J. W. Guag, and N. Kuster, "The virtual family - development of surface-based anatomical models of two adults and two children for dosimetric simultaions," *Physics in Medicine and Biology*, vol. 55, no. N23-N38, Jan. 2010. [Online]. Available: http://dx.doi.org/10.1088/0031-9155/55/2/N01

[17] S. Gabriel, R. W. Lau, and C. Gabriel, "The dielectric properties of biological tissues," *Physics in Medicine and Biology*, pp. 2231–2293, 1996. [Online]. Available: http://niremf.ifac.cnr.it/tissprop/

[18] *IEEE standard for safely levels with respect to human exposure to radiofrequency electromagnetic fields, 3 KHz to 300 GHz*, IEEE Standard C95.1, 1999.

[19] *IEEE standard for safely levels with respect to human exposure to radiofrequency electromagnetic fields, 3 KHz to 300 GHz*, IEEE Standard C95.1, 2005.

[20] *Specific Absorption Rate (SAR) for Cellular Telephones*, Federal Communication Commision (FCC), USA, 2012. [Online]. Available: http://www.fcc.gov